Deformability of red blood cells affects their velocity in deterministic lateral displacement devices

Timm KRÜGER [1,*], David HOLMES [2], Peter V. COVENEY [3]

* Corresponding author: Tel.: +44 (0)131 650 5679; Email: timm.krueger@ed.ac.uk
1: School of Engineering, University of Edinburgh, Edinburgh, UK
2: Sphere Fluidics Ltd., Cambridge, UK
3: Centre for Computational Science, University College London, UK

Abstract Recent years have witnessed a strong increase of interest in mechanical particle separation in structured microfluidic devices. Particular examples are enrichment of rare cells in blood (*e.g.* cancer cells) or separation of complex mixtures of suspended particles. In many cases, particles are separated based on their size, for example white and red blood cells (RBCs). A less common idea is deformability-based sorting of particles of the same size – an approach relevant for malaria detection where the infected RBCs are usually more rigid than their healthy counterparts. We have recently shown that the trajectories of RBCs in deterministic lateral displacement devices strongly depend on their rigidity. In the present article, we investigate – via computer simulations based on the immersed-boundary, lattice-Boltzmann and finite-element methods – the RBC velocity and show that it is significantly affected by the cells' deformability.

Keywords: Deterministic Lateral Displacement, Red Blood Cells, Deformability, Particle Separation

1. Introduction

Malaria is one of the deadliest infectious diseases accounting for about one million death cases every year (Nayyar et al., 2012). It is therefore of paramount importance to improve the efficiency of disease prevention, diagnosis and treatment.

The most common malaria diagnosis tools are microscope examinations of blood smears (which require experienced personnel) or antigen tests (which involve the use of chemicals) (Abba et al., 2011). A cheap, easy to use, portable and purely mechanical means to detect malaria-infected red blood cells would therefore be of clear advantage.

About one decade ago, a novel mechanical particle separation technique was proposed: deterministic lateral displacement (DLD) (Huang et al., 2004). The underlying idea is the excluded volume effect due to collision of particles in micro-structured arrays of pillars in a shallow flow chamber. During their passage through the device, particles can interact with the pillars *via* physical collisions which, depending on the particle size, can lead to different trajectories. While smaller particles tend to follow the streamlines on zigzag-like trajectories without net lateral displacement, larger particles can be displaced, which leads to a separation of the smaller and the larger particles.

While DLD devices have been successfully applied to separate blood components by size (Davis et al., 2006) or red blood cells (RBCs) from parasites (Holm et al., 2011), particle deformability is usually considered a detrimental effect since it generally leads to unpredictable trajectories (Al-Fandi et al., 2011).

In a recent work, we have investigated the trajectories of RBCs in DLD devices as a function of pillar row shift and particle deformability (Krüger et al., 2014). We have shown that RBCs of different deformability can be separated when the row shift and capillary number are properly chosen. In particular, this may allow for the separation of malaria-infected and healthy RBCs since the former are usually more rigid than the latter.

In the present article we focus on the average velocity of RBCs in the same DLD

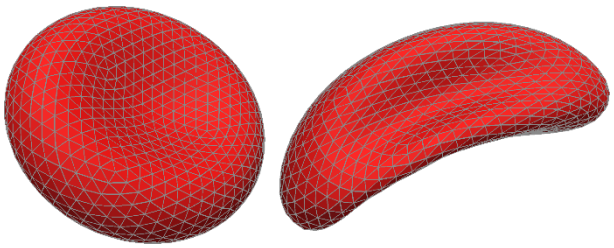

Fig. 1. Geometry of an undeformed (left) and deformed (right) red blood cell, discretised by 2,000 flat triangular elements.

setup. We show that the velocity depends strongly on the row shift and deformability. We rationalise this behaviour in terms of physical collisions of the RBCs with the pillars.

The numerical method and the simulation parameters are briefly summarised in section 2, followed by the results and discussion in section 3 and the conclusions in section 4.

2. Numerical Method and Simulation Parameters

The numerical method employed in this paper is a hybrid approach, based on the lattice-Boltzmann method (Succi, 2001) as Navier-Stokes solver, the finite-element method (Charrier et al., 1989) to capture the dynamics of the RBC membranes and the immersed-boundary method (Peskin, 2002) to provide the required bidirectional coupling of the fluid and the membrane. This algorithm has been extensively tested and documented in the past, see e.g. Krüger et al. (2011a, 2011b, 2013).

The RBC membrane has been approximated by a triangular mesh with 2,000 elements (cf. Fig. 1). Beside its shape and radius, $r = 3.9$ µm, the most important RBC parameter is its shear modulus k_s which is about 5.3 µN/m for healthy RBCs (Suresh et al., 2005).

We employ the Bhatnagar-Gross-Krook lattice Boltzmann method with 19 discrete velocities. The viscosity of the ambient liquid is tightly connected to the lattice Boltzmann relaxation parameter τ. By setting the outside and inside liquid viscosities to $\nu_{out} = 1/6$ and $\nu_{in} = 5/6$ (in simulation units), respectively, we take into account the viscosity contrast $\lambda = \nu_{in}/\nu_{out}$ which is often assumed to be around 5.

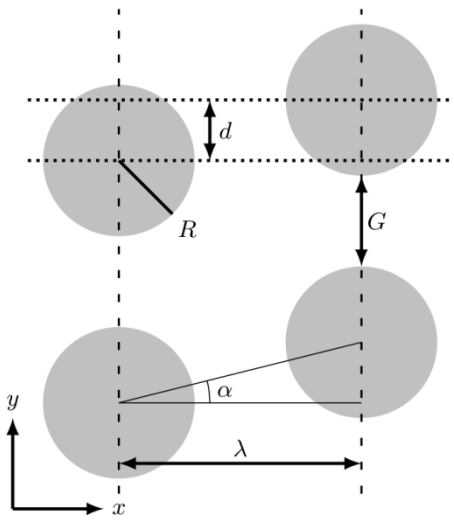

Fig. 2. Geometry of the employed deterministic lateral displacement device.

The flow is driven by a constant force density f mimicking a pressure gradient p'.

The parameters for the DLD device (cf. Fig. 2) are as follows: $R = 10\,\mu m$, $G = 12\,\mu m$, $\lambda = 32\,\mu m$. The height is $H = 4.8\,\mu m$ to enforce alignment of the RBC with the confining bottom and top walls. The row shift d is the only free geometry parameter in the present work. The spatial resolution is given by the lattice constant which is 0.4 µm in all cases.

The other free control parameter is the capillary number $Ca = \sigma r/k_s$, the ratio of the external, deforming stress $\sigma = p'\ell$ (which is given by the externally applied pressure gradient p' and the pillar gap length scale $\ell = \sqrt{GH}$) to the restoring elastic membrane stress k_s/r. Larger values of Ca indicate more strongly deformed RBCs. In practice, we vary the capillary number by changing the RBC modulus, rather than the force density. This ensures that the average liquid velocity in simulation units is the same in all our simulations, which facilitates the data analysis. For all our simulations, $f = 9.36 \cdot 10^{-5}$ (in simulation units) holds.

Since we assume the validity of the Stokes approximation, the viscous time scale is arbitrary and a conversion of simulation to physical units is possible by matching the capillary number. For example, assuming healthy RBCs with $k_s = 5.3$ µN/m, $Ca = 0.6$ leads to $\sigma = p'\ell = 0.82$ Pa and

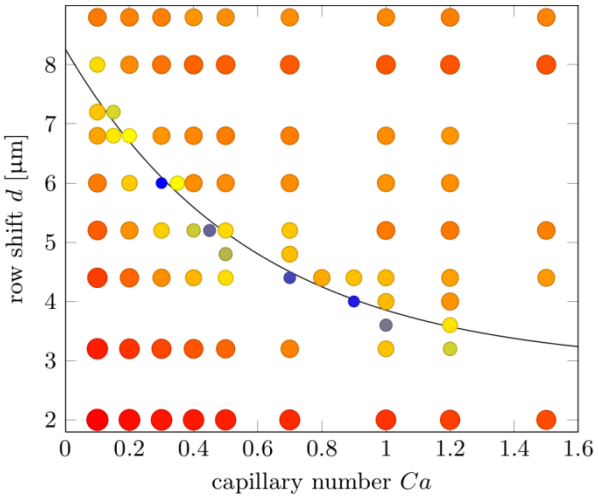

Fig. 3. Average velocity of red blood cells in the employed deterministic lateral displacement device (in arbitrary units). The circle area is proportional to the velocity. The solid line corresponds to the critical separation between displaced (below) and non-displaced (above) cells.

using $\ell = \sqrt{GH} = 7.6$ µm we obtain a pressure gradient $f = p' = 108$ kPa/m.

3. Results and Discussion

We have run a large number of simulations and varied the parameter d between 2.0 and 8.8 µm and Ca from 0.1 (relatively rigid) to 1.5 (strongly deformed). The major findings, in particular the shape of the RBC trajectories, have been investigated previously (Krüger et al., 2014). Here we focus on the velocity of the RBCs in the DLD device.

The essential results are presented in Fig. 3. The solid line corresponds to the critical separation line between displaced particles (below the line) and non-displaced particles on zigzag trajectories (above the line). The area of the circles in the figure is proportional to the average RBC velocity. Note that, due to the assumed Stokes approximation, the time scale is arbitrary and the velocity does not have to be directly converted into physical units. Such a conversion is possible after fixing either the cell elasticity or the viscosity in physical units (see above). For our discussion here, it is not necessary to convert units, though. Only relative cell velocities, expressed by the symbol size in Fig. 3, are relevant.

We observe the following trends:

1. Velocities are large for either small (< 3.2 µm) or large (> 7.2 µm) row shift d.
2. Velocities are also large for nearly rigid RBCs ($Ca = 0.1$).
3. All velocities in the vicinity of the critical separation line are significantly reduced, in the most severe case by more than a factor of 4 compared to the fastest cells. We note that even smaller velocities could be observed, but we have not attempted to detect the global minimum.

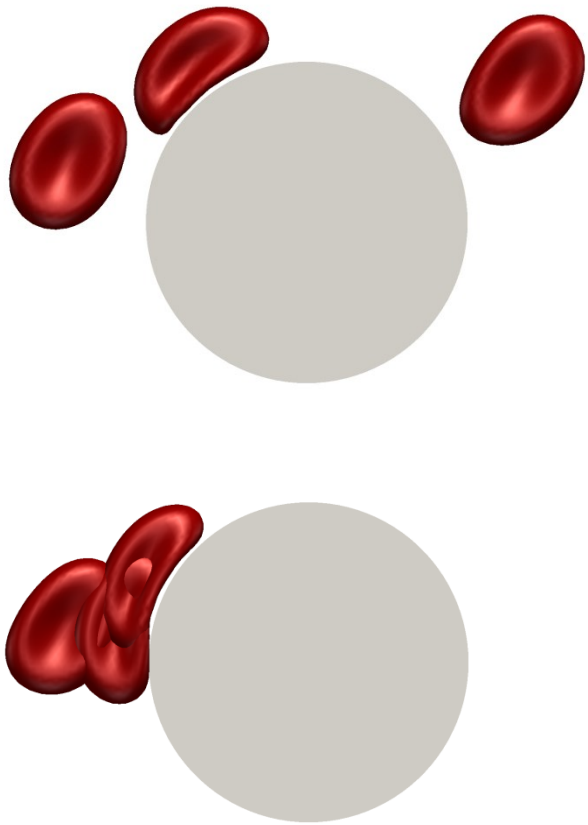

Fig. 4. Overlay sequence of red blood cells moving from left to right for $d = 4.4$ µm and $Ca = 0.5$ (top panel) and $Ca = 0.7$ (bottom panel). The interval between successive snapshots is identical (10,000 time steps).

We note that the reason for the deformability-dependence of the velocity is directly related to the physical interaction of the RBC and the pillars. RBCs far away from the critical separation line in the parameter space in Fig. 3 usually do not approach the pillars or only graze them. The smaller the distance of the chosen parameter point (Ca, d) to the critical separation line, the more strongly the RBC is affected by the pillars as rigid obstacles. Eventually, for parameters in the direct vicinity of the

separation line, RBCs tend to suffer from head-on collisions with the pillars at flow stagnation points. It then takes a long time for the cells to roll over and be dragged along by the ambient liquid. This is illustrated in Fig. 4 where the collision of two RBCs ($Ca = 0.5$ and $Ca = 0.7$) with a pillar in a DLD device with $d = 4.4$ μm is shown as a time sequence. In the former case, the RBC is grazing the pillar but does not experience a head-on collision. In contrast, in the latter case, the RBC hits the pillar directly and gets appreciably delayed. The difference in average velocity for these two cases can also be seen in Fig. 3.

These observations have the following implication: for a fixed row shift d (i.e. a given DLD device), the average RBC velocity is relatively independent of Ca far from the separation line. RBCs which are within a certain deformability window approach the pillars and are slowed down due to direct collisions with the pillar. This way, those RBCs are slower on average and should reach the device outlet after all other RBCs. This way, a pulsed operation mode should in principle allow for RBC separation within a given deformability *range* from the remaining cells. This could be relevant if there are more than two species of particles with different rigidities.

4. Conclusions

We have performed immersed-boundary-lattice-Boltzmann-finite-element simulations of red blood cells (RBCs) in a deterministic lateral displacement (DLD) device. The relevant control parameters are, on the one hand, the row shift d of the DLD setup and, on the other hand, the relative deformability of the RBCs, expressed by the capillary number Ca. This capillary number is essentially the ratio of external stresses due to the applied pressure gradient to the intrinsic RBC elastic stress.

In a previous work (Krüger et al., 2014) we have shown how the trajectories of RBCs in DLD devices depend on the row shift and capillary number. In particular, we have identified the critical separation line between displaced and non-displaced RBCs. In the latter case, the RBCs move on trajectories resembling a zigzag line.

In the present article, we focus on the average RBC velocity. The main result is that the RBC moves fastest if the row shift is either larger or significantly smaller than the RBC diameter. For row shifts comparable to the RBC diameter, the velocity strongly depends on the row shift and the capillary number. In particular, the velocity decreases dramatically when the chosen combination of d and Ca is close to the critical separation line in the $d - Ca$ diagram.

The reason for this effect is that particles close to the critical deformability approach the stagnation point at the next downstream pillar, leading to a head-on collision of the RBC and the pillar. Rolling over the pillar then takes significantly longer than sliding past the pillar as is the case for particles farther away from the critical separation line.

By following the time of arrival of those cells, the presented effect may be used to identify RBCs with a particular deformability range, rather than to separate particles above and below a specific threshold value.

Malaria-infected RBCs demonstrate a progressive stiffening of their cell membranes, as the parasite grows inside the cell. Early stage infected RBCs retain the typical biconcave morphology and have identical size to uninfected cells. Our model suggests there is significant potential for the development of low cost portable malaria diagnostic devices based on the use of DLD.

Acknowledgements

This work was supported by the EPSRC grant “Large Scale Lattice Boltzmann for Biocolloidal Systems” (Grant No. EP/I034602/1) and the EC-FP7 project CRESTA (http://www.cresta-project.eu/; Grant No. 287703). TK acknowledges the University of Edinburgh for awarding a Chancellor’s Fellowship.

References

Abba, K., Deeks, J.J., Olliaro, P.L., Naing, C.-M., Jackson, S.M., Takwoingi, Y., Donegan, S., Garner, P., 2011. Rapid diagnostic tests for diagnosing uncomplicated P. falciparum malaria in endemic countries. Cochrane Database Syst. Rev., 7.

Al-Fandi, M., Al-Rousan, M., Jaradat, M.A.K., Al-Ebbini, L., 2011. New design for the separation of microorganisms using microfluidic deterministic lateral displacement. Robot. CIM-Int. Manuf., 27, 237-244.

Charrier, J.M., Shrivastava, S., Wu, R., 1989. Free and constrained inflation of elastic membranes in relation to thermoforming – non-axisymmetric problems. J. Strain Anal. Eng., 24, 55-74.

Davis, J.A., Inglis, D.W., Morton, K.J., Lawrence, D.A., Huang, L.R., Chou, S.Y., Sturm, J.C., Austin, R.H., 2006. Deterministic hydrodynamics: taking blood apart. P. Natl. Acad. Sci. USA, 103, 14779-14784.

Holm, S.H., Beech, J.P., Barrett, M.P., Tegenfeldt, J.O., 2011. Separation of parasites from human blood using deterministic lateral displacement. Lab Chip, 11, 1326-1332.

Huang, L.R., Cox, E.C., Austin, R.H., Sturm, J.C., 2004. Continuous particle separation through deterministic lateral displacement. Science, 304, 987-990.

Krüger, T., Varnik, F., Raabe, D., 2011a. Efficient and accurate simulations of deformable particles immersed in a fluid using a combined immersed boundary lattice Boltzmann finite element method. Comput. Method. Appl., 61, 3485-3505.

Krüger, T., Varnik, F., Raabe, D., 2011b. Particle stress in suspensions of soft objects. Philos. T. Roy. Soc. A., 369, 2414-2421.

Krüger, T., Gross, M., Raabe, D., Varnik, F., 2013. Crossover from tumbling to tank-treading-like motion in dense simulated suspensions of red blood cells. Soft Matter, 9, 9008-9015.

Krüger, T., Holmes, D., Coveney, P.V., 2014. Deformability-based red blood cell separation in deterministic lateral displacement devices – a simulation study. Submitted to Lab Chip for review (http://arxiv.org/abs/1406.1877).

Nayyar, G.M.L., Breman, J.G., Newton, P.N., Herrington, J., 2012. Poor-quality antimalarial drugs in southeast Asia and sub-Saharan Africa. The Lancet, 12, 488-496.

Peskin, C., 2002. The immersed boundary method. Acta Numerica, 11, 479-517.

Succi, S., 2001. The lattice Boltzmann equation for fluid dynamics and beyond. Oxford University Press, Oxford.

Suresh, S., Spatz, J., Mills, J., Micoulet, A., Dao, M., Lim, C., Beil, M., Seufferlein, T., 2005. Connections between single-cell biomechanics and human disease states: gastrointestinal cancer and malaria. Acta Biomaterialia, 1, 15-30.